

Nuclear magnetic resonance in liquid ^3He in a volume experimental geometry

I. S. Solodovnikov and N. V. Zavaritskiĭ

Institute of Physics Problems, Russian Academy of Sciences, 117973 Moscow, Russia

(Submitted 6 June 1996)

Zh. Éksp. Teor. Fiz. **110**, 2047–2060 (December 1996)

The spin–spin relaxation times of liquid ^3He in a silica glass bulb are determined at temperatures of 0.08–0.3 K in magnetic fields of 2–44 Oe. The decrease in the magnetic moment of ^3He after exposure of the bulb to an rf field at the proton resonant frequency is also measured; it is attributable to the interaction of the spins of ^3He and protons of residual water on the glass surface. When bulk spin relaxation is taken into account, the magnetic moment of liquid ^3He nuclei in the saturation of proton NMR, normalized to the equilibrium value at the given temperature, does not depend on the temperature. © 1996 American Institute of Physics. [S1063-7761(96)00912-2]

1. INTRODUCTION

The surface magnetic properties of liquid ^3He have been studied in many papers.^{1–4} The investigations are usually carried out with porous or finely disperse materials (in experiments with a bounded experimental geometry), and natural (bulk) relaxation of the spins of liquid ^3He does not occur in this case. Measurements of the spin relaxation times of ^3He , which are surface-controlled, have been reported.^{1–4} The authors assume that the relaxation of the spins of ^3He at the wall is governed by a surface coating of solid helium; the spin relaxation rate in this coating for a dielectric substrate devoid of electron paramagnetic impurities is approximately identical for different types of walls. Recent studies^{1–4} have been devoted to the ^3He – ^{19}F system (Refs. 1–4). A number of experiments have been performed on the system ^3He – ^1H (Refs. 1,5,6).

Many liquid ^3He experiments are carried out in a “volume” experimental geometry, i.e., in an experimental chamber with characteristic dimensions ≥ 1 mm.^{6–8} The surface can also play a significant role in these experiments. The usual material of the wall of the experimental chamber is epoxy resin.^{6–8} Bunkov *et al.*⁷ have found that the surface relaxation rate in their experiments is approximately 30 times the rates calculated from the results of experiments in a bounded geometry. In Ref. 6, as in experiments in a bounded geometry, the magnetic moment of liquid ^3He was observed to decrease when the experimental cell was irradiated by a radio-frequency (rf) field at the nuclear magnetic resonance frequency of the protons of the chamber wall, owing to the interaction of ^3He – ^1H spins on the surface. On the other hand, the phenomenon exhibited a strong temperature dependence, conflicting with the results of experiments in a bounded geometry. The insufficient intensity of the rf fields at low temperatures and possible diffusion of the magnetization in the proton system from the surface into the depth of the wall make it difficult to analyze the results of Ref. 6. It is important to investigate the NMR of liquid ^3He with a better defined surface, quartz glass. To the best of our knowledge, only in the work of Gaines *et al.*⁹ in the early sixties has such a chamber been used to study the NMR of liquid ^3He . Her-

metically sealed Pyrex and silica glass bulbs have been used in experiments with gaseous ^3He (Ref. 10).

Nuclear magnetic resonance studies of helium-3 in glass chambers have demonstrated the need to clean impurities from the glass surface.^{10,11} In the reported studies the surface was cleaned by vacuuming at room or elevated temperatures and by the application of a high-frequency discharge. It is possible, however, that these methods would not be very effective in ridding the surface of heavy metal atoms or ions, which tend to exhibit a high magnetic moment of electronic origin. It is known from the literature¹² that these impurities can be removed by washing the glass with acid. We have used this surface cleaning method in the present study. It is well known that the surface of silica glass can acquire “smoky spots” with a developed surface as a result of the evaporation and condensation of silicon dioxide when the glass is melted.¹⁰ Alkali etching has been used in the present study to eliminate these zones from the surface.

2. EXPERIMENTAL PART

The bulbs were blown from industrial silica glass. They had a stem of length 12 mm and diameter 3.7 mm with an opening of diameter 0.9 mm communicating with the measurement volume (approximately 0.29 cm³), which was 15 mm long and had a middle cylindrical section of diameter 5.4 mm and a wall thickness of 0.4 mm. Smoky zones were visible on sporadic parts of the surface. The bulbs were held for 20 h in an aqueous NaOH solution with a concentration of 2.5 moles/l at a temperature of 80 °C; the tested solution was introduced into the interior of the bulbs by means of a Teflon capillary tube. The bulbs were etched and then washed in distilled water. The thickness of the dissolved alkali coating was determined from the weight loss of the bulbs and the geometrical area of the surface and had a value of about 7 μm . After alkali etching, the surfaces of the bulbs had a slightly matte appearance without any visible smoky zones. One of the two bulbs was then washed in 50% sulfuric acid for two hours at a temperature of approximately 30 °C to remove impurities, followed by a final rinse in distilled water. The main results of the study pertain to this bulb.

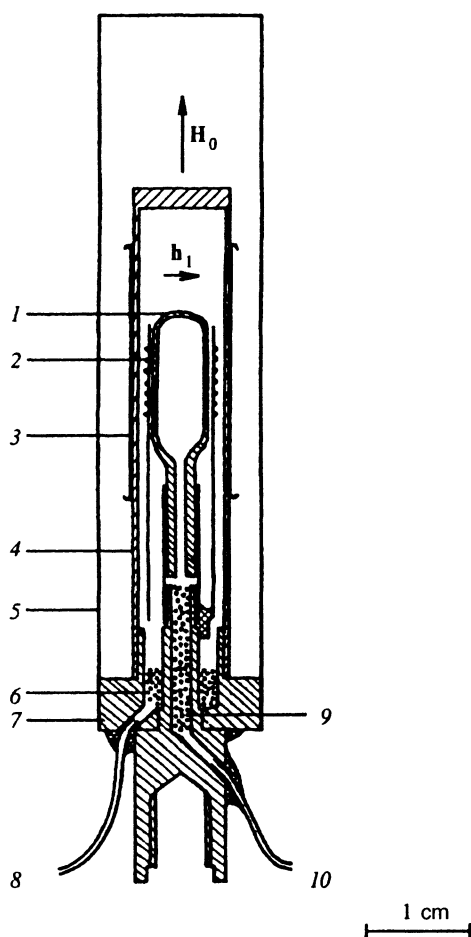


FIG. 1. Schematic view of the experimental arrangement. 1) Silica glass bulb; 2) sensing coil of a SQUID magnetometer; 3) rf field coil; 4) outer wall of the ^4He chamber; 5) cell shield of Mylar, copper, and niobium foil; 6) roasted copper powder; 7) copper cold conductor; 8) ^4He filling line; 9) pressed and roasted copper-silica gel powder; 10) ^3He filling line.

The experimental chamber is shown schematically in Fig. 1. The lower part contained a copper cold conductor wound tightly around the copper solution chamber of a ^3He - ^4He refrigerator. The line used to fill the bulb with ^3He inside the cold conductor of the chamber passed through pressed and roasted copper powder of mass 0.1 g premixed with crushed KSKG silica gel powder of mass 7 mg, which was used to absorb the ^4He impurity. The diameter of the upper part of the copper cold conductor was equal to the diameter of the stem of the glass bulb; these elements were connected by a tube of Mylar (polyethylene terephthalate, a thermoplastic polyester resin) foil with a wall thickness of about $40\ \mu\text{m}$, which was bonded to them by Stycast 1266 epoxy sealant. The glass bulb was housed in an auxiliary chamber, which could be filled with liquid ^4He to ensure good thermal contact of the ^3He inside the bulb with the copper cold conductor. Copper powder of mass 0.23 g was pressed and roasted in the interior cavity of the cold conductor in the lower part of the ^4He chamber; there it had a surface area of about $0.08\ \text{m}^2$, and a line filled with ^4He was run through it. The walls of the chamber were sealed off from the Mylar film by epoxy sealant; superconducting coils

were bonded to the outside of the upper part for the excitation of NMR. Inside the ^4He chamber the silica glass bulb was enclosed in (but not in contact with) a Mylar tube, to which the NMR sensing coil was attached. The experimental chamber was encased in a shield of Mylar, copper, and niobium foil screen rolled and welded into a tube.

The ^3He gas used to fill the cell contained about 0.02% ^4He . The difference in the adsorption energies of ^4He and ^3He is approximately 2 K (Ref. 13), which can be exploited to achieve selective absorption of the helium-4 impurity. The main filter designed for removal of the ^4He impurity was in thermal contact with the evaporation chamber of the ^3He - ^4He refrigerator (approximate temperature 0.6 K). This filter consisted of copper powder of mass 0.18 g mixed with KSKG powdered silica gel of mass 16 mg, which was pressed and roasted. The final removal of ^4He was accomplished by the roasted powder inside the cold conductor of the cell. The total volume of condensed ^3He was approximately $0.45\ \text{cm}^3$. The ^3He was condensed for 1.5–2 h; the temperature of the cell did not exceed 0.2 K in this case. The pressure of the ^3He at the end of condensation was 6 torr. Prior to the experiments the ^3He line to the experimental chamber was evacuated for 3–5 days at room temperature to a pressure below 10^{-3} torr, which was measured on the upper flange of the cryostat.

The temperature of the cell was determined by means of two resistance thermometers mounted on the copper cold conductor. One of the thermometers was the sensing element of a temperature regulator. The relaxation time to thermal equilibrium between the cold conductor and the liquid ^3He in the glass bulb was dictated by Kapitza heat transfer at the glass-helium boundaries and was estimated to be 0.5 h at $T=0.05\ \text{K}$. At the lowest temperature in our experiments, which was approximately 0.08 K, we waited 1–1.5 h before starting the measurements.

In this work the spin NMR of liquid ^3He was detected by means of a magnetometer utilizing an rf SQUID (superconducting quantum interference device).¹⁴ The superconductive sensing coil of the magnetometer surrounded the bulb containing the liquid ^3He (see Fig. 1), its sensing axis aligned with the static magnetic field H_0 (z axis), and enabled us to determine the variation of the longitudinal magnetic moment of the sample in NMR excitation. A $0.3\text{-m}\Omega$ resistance was inserted in the line from the sensing to the signal coil, shunting the inductance from the rf field. To provide additional protection from the influence of the rf field, the signal coil, which was inserted in one of the openings of the SQUID, was enclosed in a shield of bronze foil tinned with superconducting solder. The SQUID mounting had a frequency band from zero to $\sim 10\ \text{Hz}$ and was almost totally insensitive to rf fields up to $\sim 1\ \text{Oe}$ at frequencies above 20 kHz. The SQUID output was recorded on a computer.

A static magnetic field H_0 was generated by a superconducting solenoid at a cell temperature of approximately 15 K and during cooling was confined by the niobium tube of the cell shield. The rf field h_1 was generated by two crossed coils of niobium-titanium wire with a thickness of 0.04 mm. We used circularly polarized rf fields close to the NMR frequency of ^3He and the proton NMR frequency; the

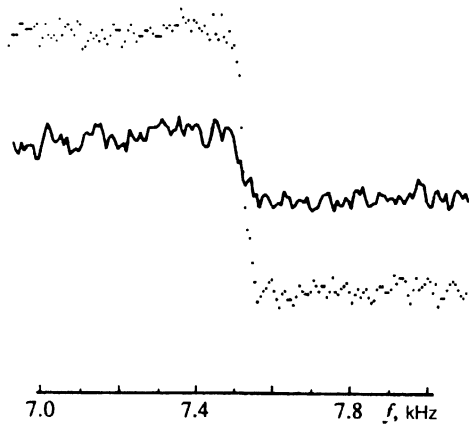


FIG. 2. Typical plot of the SQUID output for two successive passes through the resonance line. The transmission represented by the solid curve was made 240 s after the transmission represented by the dots. $H_0=2.3$ Oe, $T=0.22$ K, rf field $h_1=6$ mOe; for both plots the frequency of the rf field is swept "bottom to top" at a rate of 0.18 kHz/s.

two fields had opposite senses of rotation. Both fields could be activated simultaneously in our experiments.

To measure the equilibrium magnetic moment M_0 of the ^3He nuclei (in units of the SQUID output) and the longitudinal relaxation time T_1 , rapid adiabatic passes through the NMR were executed, accompanied by inversion (reversal) of the longitudinal magnetic moment of the sample.¹⁵ A pass across the NMR line appears in the form of steps on the plotted SQUID output; see Fig. 2. In our experiments we used pairs of such passes. The first pass initializes the sample with an inverted magnetic moment; half the step height corresponds to the quantity M_0 . Spin relaxation takes place in the time between the first and second pass. The step height in the second pass can be used to determine the magnetic moment before this pass and to calculate the longitudinal spin relaxation time T_1 . We used the procedure described in Ref. 6 to calculate T_1 ; a correction was introduced for the incomplete equilibrium of the spins prior to the first pass. The exponential law of longitudinal relaxation of the nonequilibrium magnetic moment was tested by selecting various time intervals between the first and second pass. Two to five pairs of such passes were executed at a given temperature and magnetic field. The resulting values of T_1 are shown in Fig. 3.

3. SPIN-LATTICE RELAXATION

The longitudinal spin relaxation rate can be described by the expression

$$\frac{1}{T_1} = \frac{1}{T_B} + \frac{1}{T_W + T_D}. \quad (1)$$

Here T_B is the intrinsic (bulk) spin relaxation time of liquid ^3He . The intrinsic spin relaxation time is associated with dipole-dipole interaction, which depends on the time by virtue of the motion of atoms of the liquid. The theory of the spin relaxation of liquid ^3He is discussed in Refs. 17 and 18. The time T_B is independent of the magnetic field at all fields attainable in practice. At $T \approx 0.3$ K the time $T_B(T)$ increases

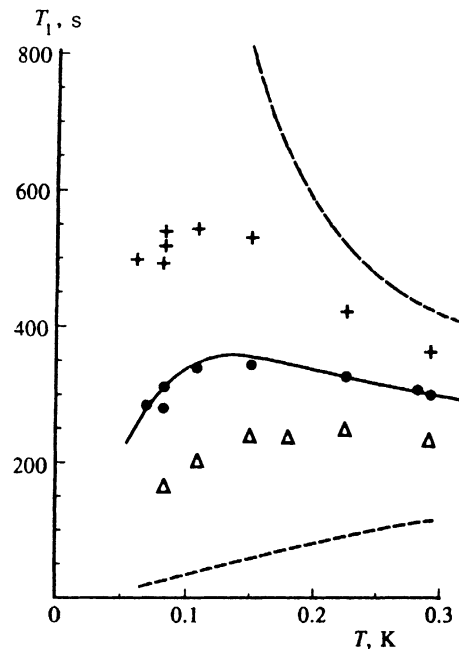


FIG. 3. Experimental values of the longitudinal relaxation time for various values of the magnetic field: Δ) 2.3 Oe; \bullet) 11 Oe; $+$) 44 Oe. Solid curve: approximation of the data for $H_0=11$ Oe by relations (1) and (2); long-dash curves in upper part of the figure: intrinsic (bulk) spin relaxation time T_B of liquid ^3He at the saturated vapor pressure^{8,16}; short-dash curve: estimated characteristic time T_D for diffusion of spins toward the bulb walls.

as the temperature drops, owing to the degeneracy of the Fermi liquid. The values of T_B at the saturated vapor pressure and at temperatures of 0.15–0.6 K are known to within roughly 5% error limits.^{8,16} The following expression has been derived¹⁶ for the time T_B determined from the longitudinal spin relaxation rate $1/T_1$ of liquid ^3He in an epoxy chamber as a function of $1/H_0$ with extrapolation to the limit $1/H_0 \rightarrow 0$:

$$T_B = 287 + \frac{11.8}{T^2}, \quad 0.15 < T < 0.6 \text{ K},$$

where T_B is expressed in seconds, and T in kelvins. A similar calculation of the time T_B at the temperature $T=0.29$ K from the values of T_1 obtained in the present study in magnetic fields $H_0=22$ Oe and 44 Oe yields the same value as in Ref. 16 to within the error of determination of the relaxation times. We have extrapolated the above expression for T_B to lower temperatures $T < 0.15$ K; at these temperatures in our experiments the spin relaxation becomes slower than at the walls. The function $T_B(T)$ is represented by the long-dash curve in Fig. 3. In expression (1) we have discarded the term associated with spin diffusion along the channel used for filling the measurement volume of the bulb. The corresponding contribution to the relaxation rate does not exceed the error associated with the uncertainty of T_B .

The second term on the right-hand side of Eq. (1) gives the spin relaxation rate at the chamber wall. The time T_D describes the diffusion of spins toward the walls. Using data from numerical simulation of the diffusion process, we have calculated T_D as $t^2/8D$, where r is the radius of the cylindri-

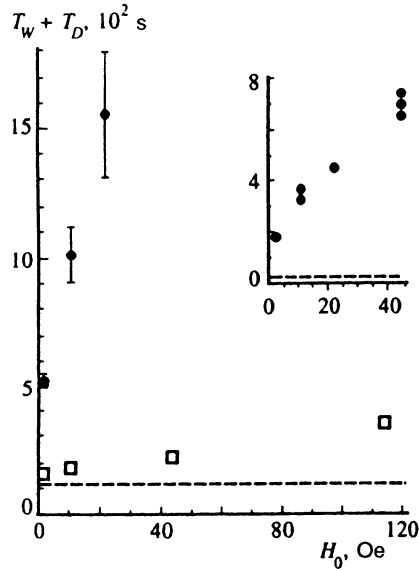


FIG. 4. Longitudinal relaxation time of liquid ${}^3\text{He}$ at the walls, equal to the sum of the wall relaxation time T_w and the spin diffusion time toward the walls T_D , at $T=0.29$ K. \square) bulb without acid washing; \bullet) bulb with a cleaned surface, showing the systematic error associated with the uncertainty with which the bulk relaxation time T_B is known. The dashed line represents an estimate of the time T_D . Inset: data for the bulb with a cleaned surface at $T=0.083$ K.

cal part of the measurement volume, and D is the spin diffusion coefficient.⁸ This estimation has a probable error of 20%. The values thus calculated for T_D are represented by the dashed curve in the lower part of Fig. 3.

The quantity T_w in expression (1) gives the longitudinal spin relaxation time directly at the walls. For the bulb prepared with an acid wash we have $T_w > 4T_D$. Only the time T_w can depend on the magnetic field on the right-hand side of expression (1).

The values of $T_w + T_D$ are calculated according to relation (1) from the experimentally determined values of T_1 at the two temperatures $T=0.29$ K and $T=0.083$ K. These data are shown in Fig. 4 as a function of the static magnetic field H_0 . In the case of the bulb whose surface was not acid-washed the value of T_w at $H_0 < 40$ Oe is lower than T_D , so that in light of the uncertainty of estimation of T_D we do not distinguish the time T_w explicitly. It is evident from Fig. 4 that acid washing of the surface increases the wall relaxation time by roughly an order of magnitude. This increase is probably attributable to the removal of surface impurities, which accelerate spin relaxation. The influence of surface paramagnetic ions on the spin relaxation of ${}^3\text{He}$ has been studied in previous experiments.¹⁹ In the case of the bulb with the cleaned surface the time T_w depends almost linearly on the magnetic field H_0 ; as H_0 is decreased, T_w approaches a value much greater than the time T_D .

According to the usual model^{1,4} proposed by Hammel and Richardson,²⁰ the wall spin relaxation of liquid ${}^3\text{He}$ is determined by a surface coating of solid helium. Relaxation is attributable to the temperature-independent exchange motion of atoms of this coating, which modulates the dipole-dipole interaction between ${}^3\text{He}$ nuclei and also between

${}^3\text{He}$ spins and the nuclear spins of wall atoms. The temperature dependence of the wall spin relaxation time as predicted by this model well describes the results of measurements of this quantity in experiments with a bounded geometry²¹:

$$T_w = T_S \frac{N_L}{N_S} T_{\chi_L} \quad \text{for } N_L \gg N_S. \quad (2)$$

Here χ_L is the magnetic susceptibility of liquid ${}^3\text{He}$ nuclei in units of the constant in the Curie-Weiss law,^{2,22,23} N_L/N_S is the ratio of the numbers of atoms in the liquid volume and in the solid helium coating on the walls, and T_S is the temperature-independent longitudinal relaxation time of this layer. We have determined $T_S(N_L/N_S)$ with the experimental data for T_1 approximated by relations (1) and (2). The temperature dependence of the longitudinal relaxation time T_1 , calculated from relations (1) and (2) and represented by the solid curve in Fig. 3, exhibits good correspondence with the experimental data. We shall assume below that the area of the walls of the measurement volume of the bulb is equal to the geometrical area (2.4 cm²). We assume that the surface density of the solid coating on the walls is equal to the density of the monolayer formed in the adsorption of ${}^3\text{He}$ on porous Vycor glass²⁴: 0.105 atom/Å². A calculation of the time T_S for $H_0=11$ Oe in this case gives $T_S(H_0=11 \text{ Oe}) = 0.9$ ms. The dependence of T_S on the magnetic field is illustrated by the inset to Fig. 4: $T_S \propto T_w \gg T_D$ at $T=0.083$ K. The time T_S increases almost linearly with H_0 , but as H_0 is decreased, T_S approaches the value $T_S(H_0 \rightarrow 0) \approx 0.4$ ms; the same value has been obtained previously for an epoxy resin wall. A theoretical interpretation of the linear field dependence of the spin-lattice relaxation time at the walls, observed for various types of substrates, has been offered by Cowan.²⁵

The proportionality factor between T_S and H_0 in strong magnetic fields can be estimated from the slope of the $T_S(H_0)$ curve at $T=0.083$ K: $T_S/H_0 = 3 \times 10^{-5}$ s/Oe. For porous Vycor glass a value of 7.6×10^{-5} s/Oe is given in Ref. 25. According to other data,²⁶ the value of this factor for porous glass is 1.1×10^{-4} s/Oe. The porous glasses used in these papers were almost pure silica glass.

The smaller values of T_S calculated for our conditions from the geometrical area of the walls suggest that the effective surface could be ~ 3 times the geometrical surface. Other explanations are certainly possible. In porous glasses the thickness of the liquid ${}^3\text{He}$ coating is of the order of atomic dimensions. Under our conditions with a thick layer of liquid present near the wall, as mentioned in Ref. 27, another possible cause of the deviation of our value of T_S/H_0 from the data for porous glasses is that the relaxation time depends on the relative orientation of the surface and the magnetic field.²⁵ In our situation the principal surface area is associated with the side walls of the cylindrical part of the measurement volume of the bulb, where the field H_0 is parallel to the surface. In the porous glass experiments the relaxation rate is averaged over all possible orientations of the surface.²⁵

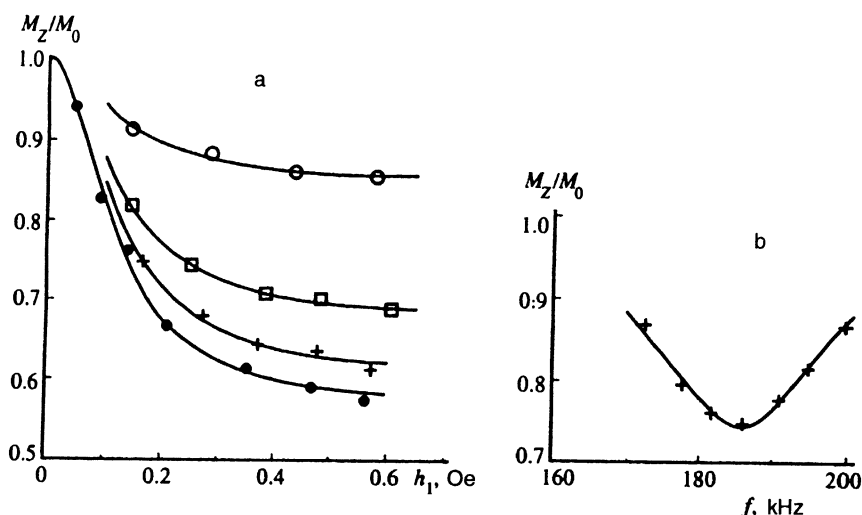


FIG. 5. Static magnetic moment of ^3He when the cell is exposed to an rf field h_1 at a frequency close to proton resonance. a) Dependence on the rf field at various temperatures ($H_0=43.6$ Oe, frequency of rf field 185.8 kHz): (●) $T=0.083$ K; (+) 0.11 K; (□) 0.15 K; (○) 0.29 K. The curves approximating these points are calculated from relation (3). b) Dependence on the frequency of the rf field ($H_0=43.6$ Oe, $h_1=0.17$ Oe; $T=0.11$ K). A Lorentzian is approximately fitted to these points.

4. INTERACTION OF THE SPINS OF ^3H - ^1H NUCLEI AT THE WALLS

In the experiments with the acid-washed bulb, as in previous work,^{6,28} we observed that the application of a continuous, circularly polarized rf field h_1 at the proton NMR frequency causes the magnetic moment of liquid ^3He to decrease. As a result of the different directions of rotation of the rf field for the magnetic resonance of protons and ^3He and the 1.3-fold difference in the resonance frequencies for these nuclei, the applied field h_1 was tuned far away from the NMR frequency of ^3He and could not have exerted a direct influence on the magnetic moment of ^3He . The decrease in the magnetic moment is attributable to the presence of chemically bound water left on the glass surface after evacuation.^{5,12} To measure the magnetic moment of ^3He , the circularly polarized rf field h_1 was applied continuously for a period of time $\approx 2T_1$; while this field was left on, an rf field at close to the NMR frequency of ^3He was then applied (usually with an intensity of approximately 25 mOe), and rapid adiabatic pass through the ^3He resonance line was executed. The longitudinal magnetic moment M_z of the ^3He nuclei could be determined from the SQUID output plotted during this pass. Pairs of such passes (Fig. 2) could be used to measure the longitudinal spin relaxation time of ^3He in the presence of the rf field h_1 .

Plots of the magnetic moment of ^3He as a function of the circularly polarized rf field applied at the proton NMR frequency are shown in Fig. 5a, in which M_0 is the equilibrium magnetic moment at the given temperature without the rf fields. We approximate the $M_z(h_1)$ curves by the relation

$$\frac{M_z}{M_0} = \frac{1 + aR h_1^2}{1 + a h_1^2}. \quad (3)$$

The quadratic dependence on h_1 describes the rf field power absorbed by the proton system of a thin layer of hydrogen atoms on the glass surface. As h_1 is increased, the magnetic moment reaches a plateau, which is determined by the value

of R . In view of the risk of possible heating of the sample of a continuous alternating field, the maximum values of h_1 in our experiments were about $4/\sqrt{a}$.

In the case of the bulb without an acid-washed surface we did not observe any changes in the magnetic moment of the sample. At the temperature $T=0.35$ K in static magnetic fields $H_0=11$ Oe and 44 Oe and in rf fields h_1 varied from zero to 0.8 Oe we obtain $M_z(h_1)/M_0=1.00 \pm 0.02$ for this bulb. Impurities are most likely present on the surface of the walls in this case, providing the main contribution to the spin relaxation of ^3He at the walls. The influence of these impurities far exceeds the contribution associated with the dipole-dipole interaction of ^3He - ^3He and ^3He - ^1H spins. Heating of the proton spin system by the rf field under such conditions does not produce any change in the magnetic moment of ^3He .

Figure 5b shows the dependence of the magnetic moment on the frequency at which the rf field h_1 is applied. This curve shows the profile of the proton NMR line. The half-width of the curve (at the half-maximum) for $H_0=44$ Oe is equal to 14 kHz. This value is smaller than the half-width of the NMR line in the case of epoxy resin (16.5 kHz; Ref. 16) and silica gel with water added (24.5 kHz; Ref. 28), but is much greater than the half-width of the line in the case of desiccated silica gel (6 kHz; Ref. 28). This result could imply the incomplete removal of physically adsorbed water from the sample surface during evacuation under our conditions.

The values of R obtained with the $M_z(h_1)$ curves approximated by relation (3) are shown in Fig. 6. The values of R increase with both the temperature and the magnetic field. The standard model for the interaction of the spins of ^3He nuclei and the nuclear spins of the substrate^{1,2,4} postulates that this interaction, like the spin relaxation of liquid helium-3, is caused by the exchange motion of ^3He atoms in the solid coating on the surface. This model predicts that R will not depend on the temperature in experiments to measure the magnetic moment of ^3He in resonant saturation of the nuclear spins of the walls in the case of a bounded ex-

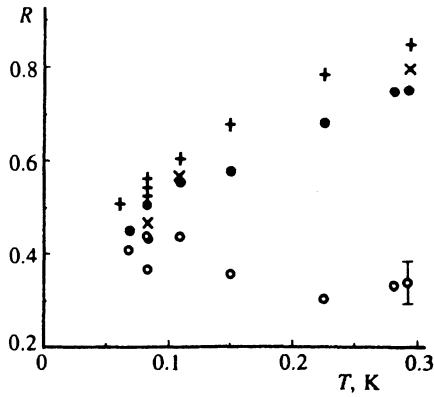


FIG. 6. Relative magnetic moment of ^3He in total saturation of proton resonance by an rf field. (●) $H_0=11$ Oe; (×) 22 Oe; (+) 44 Oe; (○) results of the calculation of R_W from Eq. (9) for $H_0=11$ Oe. The systematic error associated with the uncertainty of the time T_B is shown for the point with $T=0.29$ K.

perimental geometry. In a three-dimensional geometry a major contribution is created by the intrinsic spin relaxation of liquid ^3He . In experiments to measure the magnetic moment of liquid ^3He in the presence of NMR saturation of wall protons by the rf field, bulk relaxation diminishes the deviation of the magnetic moment M_Z from the equilibrium value M_0 and causes R to increase. The contribution of the bulk relaxation mechanism relative to the wall contribution (of order T_W/T_B) increases with the temperature and the magnetic field. Consequently, the inclusion of intrinsic spin relaxation of liquid ^3He corresponds to the observed dependence $R(T, H_0)$.

We attempt to determine qualitatively the influence of bulk relaxation on the value of R . We assume that resonance saturation of the proton system in the case of deactivated bulk relaxation changes the relative magnetic moment of ^3He M_Z/M_0 to R_W . We calculate the values of R_W , using data for R and the longitudinal relaxation times. The relaxation of the longitudinal magnetic moment in the presence of an rf field saturating proton resonance can be described by the equation

$$\frac{dM_Z}{dt} = \frac{M_0 - M_Z}{T_B} + \frac{M_0 R_W - M_Z}{T_{WSP} = T_D}. \quad (4)$$

The first term on the right-hand side describes the bulk relaxation of the magnetic moment to the equilibrium value M_0 , the second term describes the relaxation at the chamber walls to the value $M_0 R_W$, and T_{WSP} is the longitudinal wall relaxation time in the presence of proton resonance saturation; this time can differ from T_W . Under steady-state conditions we have $DM_Z/dt=0$ and $M_Z=RM_0$; in this case we obtain from (4)

$$R_W = R - (1-R) \frac{T_{WSP} + T_D}{T_B}. \quad (5)$$

According to Eq. (4), the longitudinal spin relaxation rate of ^3He in proton resonance saturation is

$$\frac{1}{T_{1SP}} = \frac{1}{T_B} + \frac{1}{T_{WSP} + T_D}. \quad (6)$$

From Eqs. (5) and (6) we obtain

$$R_W = R - (1-R) \frac{T_{1SP}}{T_B - T_{1SP}}. \quad (7)$$

Once the longitudinal relaxation time T_{1SP} of liquid ^3He has been measured in the presence of an rf field saturating proton resonance, R_W can be calculated from R according to relation (7).

We now discuss the variation of the longitudinal spin relaxation time of ^3He with the application of an rf field at the magnetic resonance frequency of the surface nuclei. We characterize the variation of the wall relaxation time by the dimensionless quantity

$$\alpha = \frac{1 - T_{WSP}/T_W}{1 - R_W}. \quad (8)$$

We consider the case of a thick (much greater than atomic dimensions) layer of liquid ^3He near the wall and a thin layer of hydrogen on the surface. The interaction model postulating a connection between the Zeeman reservoirs of ^3He and substrate nuclei through electron paramagnetic centers (Ref. 2, model A) gives $\alpha=1$. The model for the interaction of ^3He spins and surface nuclei through the dipole-dipole interaction between them, this interaction being modeled by the exchange motion of ^3He atoms in the first wall layer [Refs. 1, 2 (model B), and 4], appears to be generally accepted for the system consisting of liquid ^3He + dielectric wall without electronic impurities. In the case of weak magnetic fields, for which the Zeeman frequencies are lower than the frequency of atomic motion of the ^3He surface layer, this model predicts^{1,4}

$$\alpha = \frac{1}{2} |\gamma_{\text{He}}/\gamma_p| = 0.38.$$

In the case of strong magnetic fields it gives

$$\alpha = |\gamma_{\text{He}}/\gamma_p| = 0.76,$$

where γ_{He} and γ_p are the gyromagnetic ratios of helium-3 and protons. We note that according to these models α does not depend on the degree of saturation of the proton resonance, and here T_{WSP} and R_W are interpreted as the wall relaxation time and the steady-state relative magnetic moment (without a bulk relaxation contribution) in the presence of a given rf field h_1 .

To determine α , we have measured the longitudinal relaxation time T_{1SP} at the temperature $T=0.083$ at which the relation $T_D \ll T_1 \approx T_W \ll T_B$ holds. Under these conditions it follows from relations (1) and (6)–(8) that

$$\alpha \approx \frac{1 - T_{1SP}/T_1}{1 - R} \left(1 + \frac{T_D}{T_1} \right).$$

The corrections in the calculation of α for the diffusion of spins toward the walls and for bulk relaxation are found to be small. In calculating α , we adopt the ratio M_Z/M_0 for R , where M_Z is the steady-state magnetic moment of ^3He in the

TABLE I.

| H_0 , Oe | T , K | h_1 , Oe | $h_1\sqrt{a}$ | M_Z/M_0 | T_{1SP}/T_1 | α |
|------------|---------|------------|---------------|-------------------|-------------------|-----------------|
| 11 | 0.28 | 0.75 | 3.7 | 0.756 ± 0.005 | 0.916 ± 0.010 | 0.39 ± 0.06 |
| 11 | 0.083 | 0.74 | 3.7 | 0.463 ± 0.004 | 0.755 ± 0.014 | 0.50 ± 0.03 |
| 22 | 0.083 | 0.57 | 3.8 | 0.503 ± 0.003 | 0.760 ± 0.006 | 0.51 ± 0.02 |
| 44 | 0.083 | 0.53 | 4.5 | 0.561 ± 0.002 | 0.768 ± 0.002 | 0.55 ± 0.01 |

presence of the rf field h_1 . The results of measurements and calculations of α by means of relations (1) and (6)–(8) are summarized in Table I.

The quantity $h_1\sqrt{a}$, where a is given by relation (3), characterizes the degree of saturation of the proton resonance. The error of determination of α indicated in Table I is calculated from the errors in determining of M_Z/M_0 and T_{1SP}/T_1 . At $T=0.083$ K the quantity α increases slightly, within the measurement error limits, as the magnetic field H_0 is increased, and it corresponds to the case of intermediate magnetic fields in the spin interaction model of Refs. 1 and 4. At the temperature $T=0.28$ K the times T_D , T_W , and T_B are comparable: Spin diffusion toward the walls and bulk relaxation play a significant role; the result for α at this temperature is probably only an approximate estimate.

We know of only one paper³ in which measurements of the spin relaxation time of ^3He in the saturation of ^{19}F NMR in finely dispersed Teflon are reported; no variation of the relaxation time was observed (see Ref. 3, Fig. 12).

To ascertain the influence of bulk relaxation on R , we calculate R_W on the assumption that α does not depend on the temperature. From Eqs. (5) and (8) we obtain

$$R_W = \frac{R - (1-R)[T_W(1-\alpha) + T_D]/T_B}{1 + (1-R)T_W\alpha/T_B}, \quad (9)$$

where the relaxation time T_W directly at the walls is calculated from the longitudinal relaxation time T_1 according to relation (1). The result of calculating T_W for a field $H_0=11$ Oe is shown in Fig. 6. The gradual decrease of R_W with increasing temperature can be linked to the error in determining of the time T_W as a result of the uncertainty with which the bulk relaxation time T_B is known. Calculations for the cases $H_0=22$ Oe and 44 Oe give close values of R_W , but the error in calculating the wall spin relaxation time at high temperatures increases for these values of the magnetic field.

On the whole, after the bulk relaxation contribution has been eliminated, the result of determining the relative magnetic moment ^3He in the presence of an rf field that saturates proton resonance is found to depend weakly on the temperature. This behavior is consistent with the adopted model for the interaction of ^3He spins and substrate nuclear spins.

We now examine the results obtained in Ref. 6 from measurements of the magnetic moment of ^3He in the presence of proton NMR saturation at the walls of an epoxy resin chamber. We calculate the relative magnetic moment of ^3He for total proton resonance saturation, i.e., R , from the $M_Z(h_1)$ curves obtained in Ref. 6, using the quadratic dependence on h_1 given in (3). We then determine the values of R_W from relations (1) and (9), using the values of T_1 obtained in the experiments of Ref. 6 for $H_0=11$ Oe and the

value $\alpha=0.5$ found in the present study. The values of T_W obtained for $H_0=11$ Oe range from 0.3 to 0.4 at temperatures of 0.05–0.6 K. Consequently, the strong temperature dependence of R obtained in Ref. 6 can be attributed to the influence of bulk relaxation (as in the present study) and also to the error in determining R at low temperatures as a result of the small values of h_1 and the uncertainty of the calculation of R from the $M_Z(h_1)$ curves, owing to diffusion of the magnetization in the proton system into the interior depth of the walls.

Let us compare the values of R_W obtained in the present study with the data of Refs. 1 and 28. Van Keuls *et al.*¹ have used a mixture of polystyrene powders containing ^1H nuclei and Teflon with approximately equal surface areas. At $H_0=1.5$ kOe the relative magnetic moment of ^3He in the saturation of the proton resonance was ≈ 0.5 for five monolayers of liquid ^3He and 0.8 in the case of pores filled with liquid ^3He . The presence of Teflon powder, on whose surface the magnetic moment relaxes to the equilibrium value, unquestionably raises the values of R in Ref. 1.

In the system consisting of liquid ^3He + porous silica we have previously²⁸ obtained $R_W=0.8$ in the case of desiccated silica and $R_W=0.55$ for silicon with water added at $H_0=22$ Oe and 44 Oe. As mentioned in Ref. 28, there is a possible contribution from electron paramagnetic impurities (particularly for the desiccated sample), which has the effect of increasing the values of R_W .

5. CONCLUSIONS

We have investigated the NMR of liquid ^3He in a silica glass cell. We have measured the longitudinal magnetic relaxation times. Under our conditions spin relaxation is determined both by the bulk contribution and by the influence of the chamber walls. The temperature dependence of the wall relaxation time is well described by the Hammel–Richardson model,²⁰ which postulates that spin relaxation at the walls is associated with the exchange motion of atoms of the first ^3He layer on the surface. When the cell is exposed to an rf field at the proton NMR frequency, the magnetic moment of the ^3He nuclei is observed to decrease. We have also observed a decrease in the longitudinal spin relaxation time of ^3He in the saturation of the proton resonance by an rf field. Allowance for the influence of natural (bulk) relaxation of liquid ^3He imparts a weak temperature dependence to the relative magnetic moment of ^3He in the presence of the saturation of proton resonance by an rf field. On the whole, our data obtained for a volume experimental geometry agree with previous notions^{1,4,20,25} about the liquid ^3He –wall interface, based on the results of experiments in a bounded geometry.

This work received financial support under Project No. 244 of the State Scientific–Technical ‘‘Fundamental Metrology’’ Program.

¹F. W. Van Keuls, R. W. Singerman, and R. C. Richardson, *J. Low Temp. Phys.* **96**, 103 (1994).

²A. Schuhl, F. B. Rasmussen, and M. Chapellier, *J. Low Temp. Phys.* **57**, 483 (1984).

³L. J. Friedman, T. J. Gramila, and R. C. Richardson, *J. Low Temp. Phys.* **55**, 83 (1984).

- ⁴Q. Geng, M. Olsen, and F. B. Rasmussen, *J. Low Temp. Phys.* **74**, 369 (1989).
- ⁵O. Gonen, P. L. Kuhns, C. Zuo, and J. S. Waugh, *J. Magn. Resonance* **81**, 491 (1989).
- ⁶I. S. Solodovnikov and N. V. Zavaritskiĭ, *JETP Lett.* **56**, 162 (1992).
- ⁷Yu. M. Bunkov, V. V. Dmitriev, Y. M. Mukharsky, and D. A. Sergatskov, *Physica B* **178**, 181 (1992).
- ⁸H. Godfrin, G. Frossati, B. Hebral, and D. Thoulouze, *J. Phys. Colloq.* **41**, C7-25 (1980).
- ⁹J. R. Gaines, K. Luszczynski, and R. E. Norberg, *Phys. Rev.* **131**, 901 (1963).
- ¹⁰V. Lefevre-Seguin and J. Brossel, *J. Low Temp. Phys.* **72**, 165 (1988).
- ¹¹E. P. Horvitz, *Phys. Rev. A* **1**, 1708 (1970).
- ¹²R. K. Iler, *Chemistry of Silica, Solubility, Polymerization, Colloid and Surface Properties, and Biochemistry*, Wiley, New York (1971).
- ¹³C. P. Lusher, M. F. Secca, and M. G. Richards, *J. Low Temp. Phys.* **72**, 71 (1988).
- ¹⁴O. V. Lounasmaa, *Experimental Principles and Methods Below One Degree Kelvin*, Academic Press, New York (1974).
- ¹⁵A. Abragam, *The Principles of Nuclear Magnetism*, Clarendon Press, Oxford (1961).
- ¹⁶I. S. Solodovnikov, *Dissertation for the Degree of Candidate of Physico-mathematical Sciences* [in Russian], Inst Fiz. Probl. Ross. Akad. Nauk, Moscow (1994).
- ¹⁷D. Vollhardt and P. Wolfle, *Phys. Rev. Lett.* **47**, 190 (1981).
- ¹⁸K. S. Bedell and D. E. Meltzer, *J. Low Temp. Phys.* **63**, 212 (1986).
- ¹⁹V. V. Naletov, M. S. Tagirov, D. A. Tayurskiĭ, and M. A. Teplov, *Zh. Éksp. Teor. Fiz.* **108**, 577 (1995) [*JETP* **81**, 311 (1995)].
- ²⁰P. C. Hammel and R. C. Richardson, *Phys. Rev. Lett.* **52**, 1441 (1984).
- ²¹A. Schuhl, S. Maegawa, M. W. Meisel, and M. Chapellier, *Phys. Rev. B* **36**, 6811 (1987).
- ²²B. T. Beal and J. Hatton, *Phys. Rev.* **139A**, 1751 (1965).
- ²³H. Ramm, P. Pedroni, J. R. Thompson, and H. Meyer, *J. Low Temp. Phys.* **2**, 539 (1970).
- ²⁴D. J. Creswell, D. F. Brewer, and A. L. Thomson, *Phys. Rev. Lett.* **29**, 1144 (1972).
- ²⁵B. P. Cowan, *J. Low Temp. Phys.* **50**, 135 (1983).
- ²⁶Y. Kondo, T. Mizusaki, A. Hirai *et al.*, *J. Low Temp. Phys.* **75**, 389 (1989).
- ²⁷T. J. Gramila, F. B. Van Keuls, and R. C. Richardson, *Physica B* **165–166**, 695 (1990).
- ²⁸I. S. Solodovnikov and N. V. Zavaritskiĭ, *Zh. Éksp. Teor. Fiz.* **106**, 489 (1994) [*JETP* **79**, 267 (1994)].

Translated by James S. Wood